Probing the Potential Landscape Inside a Two-Dimensional Electron Gas

J. J. Koonen, H. Buhmann, and L. W. Molenkamp
Physikalisches Institut, Universität Würzburg, Am Hubland, 97074 Würzburg, Germany
(Received 23 April 1999)

We report direct observations of the scattering potentials in a two-dimensional electron gas using electron-beam diffraction experiments. The diffracting objects are local density fluctuations caused by spatial and charge-state distribution of donors in the GaAs-(Al,Ga)As heterostructures. The scatterers can be manipulated externally by sample illumination or by cooling the sample down under depleted conditions.

PACS numbers: 71.55.Eq, 72.20.Fr

The high electron mobilities that can be obtained in the two-dimensional electron gas (2DEG) in GaAs-$Al_xGa_{1-x}As$ heterostructures continue to fascinate the community [1,2]. At low temperatures the mobility of electrons in a perfect 2DEG is limited by ionized donor scattering. The donors are located in the doping layer, some tens of nanometers away from the 2DEG. Because of the random distribution of donor atoms, the scattering potential is not homogeneous [3]. However, there are theoretical [4] and experimental [5,6] indications that spatial correlations between donors in different charge states reduce the ionized donor scattering and thus enhance the mobility.

These different charge states exist because for structures with a certain content of Al ($x \geq 0.2$) the electronic ground state of the Si donor is twofold [7–9]: First, a shallow donor state, which is associated with a normal substitutional lattice site and a binding energy of $\approx$7 meV ($d^0 \Rightarrow d^+ + e$). Second, a more localized, deep donor level with a binding energy of $\approx$160 meV, the DX center, which derives from lattice distortions at or near the donor site. In fact, the latter is a negatively charged donor state, DX^-. At low temperatures ($T < 130$ K) DX^- states become stable against thermal dissociation ($DX^- \Leftrightarrow d^0 + e$).

Several aspects of the high mobility of a 2DEG can now be explained by invoking spatial correlations between donors in different states, d^+ and DX^- [5,6], where the roughening of the potential caused by donors in one state is effectively screened by donors in the other state. The electrostatic interaction should lead to regions of several tens of nanometers in diameter where all the donors are in one state [4], which then lead to regions of different density in the 2DEG below the donors [3,4]. The correlations can be altered externally by sample illumination [7,10,11], causing a dissociation of DX^- centers ($E_{\text{excite}} \geq 1.2$ eV) and "bias cooling," i.e., cooling the sample down while the 2DEG is depleted by an applied gate voltage [6,12–14] (this prevents DX^- formation). In experiments performed so far [5,6], the mobility of a 2DEG was inferred from standard bulk conductivity measurements probing an averaged scattering potential, which do not yield information about the local distribution of shallow donors and DX centers. Moreover, the evidence for the occurrence of donor correlations is only indirect.

In this paper we use a collimated electron beam, injected and detected via quantum point contacts (QPC), as a local probe for the scattering potentials in a 2DEG, which are due to density fluctuations caused by the donor state correlations. The observed interference patterns are analyzed using a theoretical model based on a technique developed by Saito *et al.* [15], extended to the situation where impurities are present. This model allows for a deduction of sizes and locations of the scattering potentials. Experimentally, the donor configurations are changed by illumination and bias-cooling techniques.

For the experimental investigations, several gate-defined nanostructures fabricated from conventional GaAs-$Al_{0.33}Ga_{0.67}As$-heterojunction material are used. The relevant part of the layer structure consists of 400 nm undoped GaAs, 20 nm undoped $Al_{0.33}Ga_{0.67}As$ (spacer layer), 38 nm 1.33×10^{18} cm^{-3} Si-doped $Al_{0.33}Ga_{0.67}As$, and 17 nm undoped GaAs (cap layer). Typical values for the carrier density and mobility are $n = (1.5–2.3) \times 10^{15}$ m^{-2} and $\mu = 60–150$ m^2 (V s)$^{-1}$. A schematic top view of a typical gate structure is given in Fig. 1a. Schottky gates form two opposite QPCs (injector and detector), separated by a distance of typically $L = 4$ μm. In some samples the area in between the QPCs is partly covered by an additional Schottky gate (light grey regions, Fig. 1a). The conductance of the QPC can be adjusted in such a way that only N conducting modes are transmitted ($N = Gh/2e^2$). An electrostatically defined QPC can be used as the source of a narrow electron beam which propagates in the 2DEG [16]. Any object, impurity, potential fluctuation, etc., in the path of that beam leads to spatial modifications of the beam's wave function (diffraction) and therefore to distinct interference patterns in the area behind this object, analogous to optical diffraction experiments. To detect the electronic interference patterns a second QPC in a certain distance L, smaller than the ballistic mean free path, is used. A weak magnetic field applied perpendicular to the electron propagation plane will deflect the electron beam and therefore allows one to monitor the electron-beam profile (interference patterns)

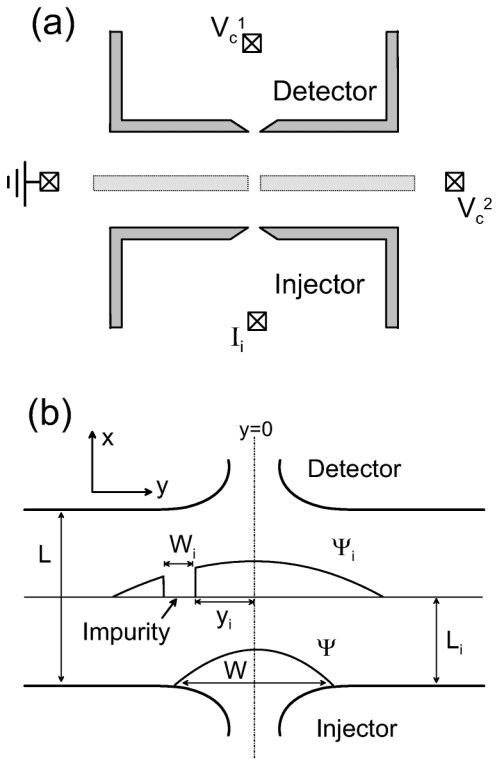

FIG. 1. Schematic view of the sample: (a) shows the gate structure and Ohmic contacts (crossed squares) of the device. Dark grey: QPC gate; light grey: optional gate used for the bias-cooling experiment; (b) defines lengths and the coordinate system and displays the electron beam wave function Ψ at the exit of the injector QPC and after impurity scattering, Ψ_i.

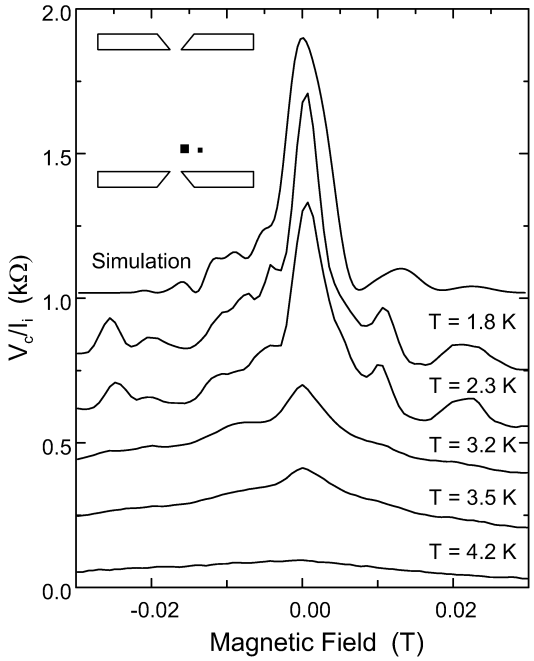

FIG. 2. Nonlocal magnetoresistance at different temperatures. A simulation of the experimental result (at 1.8 K) is obtained for a scatterer configuration indicated schematically in the top left corner: $L_{i,1} = 0.6\ \mu$m, $0.1 \le y_i \le 0.2\ \mu$m and $L_{i,2} = 0.6\ \mu$m, $0.4 \le y_i \le 0.42\ \mu$m, respectively.

in the vicinity of the detector QPC [16]. A small, low frequency ac voltage ($V_{ex} \approx 100\ \mu$V, 13 Hz) is applied to the Ohmic contacts I_i, injecting an electron beam into the 2DEG. Lock-in techniques are used to measure the voltage drop, V_c, over the detector QPC (contacts: V_c^1 and V_c^2) as a function of magnetic field. Experimentally, the measured beam profile is not smooth, but rather exhibits additional structure (see Figs. 2, 3, 4, and Ref. [16], Fig. 1). Also other groups [17,18] presented data exhibiting these features, but their origin has not been discussed previously.

In the experiments, the samples were cooled down to 1.8 K and the QPC transmittance was adjusted to $N = 1$ for injector and detector. [Injection and detection of more than one electronic mode leads to a convolution of different electronic wave functions (one for each mode) and therefore to a smearing of the observed interferences.] The opening angle of the beam could then be determined [16] to be $\approx 18°$. Figures 2, 3, and 4 show typical examples of measured nonlocal magnetoresistances. The observed structures are attributed to electron interference effects because of their marked temperature dependence (cf. Fig. 2). The interference patterns are stable in time and characteristic for a given sample. Between different cooling cycles the interference pattern changes only rarely. This is in strong contrast with typical observations on electronic quantum interferences, e.g., universal conductance fluctuations (UCF). UCFs are related to electron scattering with single impurities, whose "fingerprint" varies strongly from cooldown to cooldown, while in high-mobility 2DEGs scattering is due to random potential fluctuations, which depend on the much more robust spatial charge correlations of donors. Also, since UCFs are usually observed in a multimode regime, the amplitude of the fluctuations is much smaller than the almost 100% fluctuations discussed here.

In order to substantiate our interpretation of the experimental observations, we now model the experimentally found diffraction patterns to gain information about size and location of scattering potentials. We use the simplest possible model, based on an extension of the method of Saito *et al.* [15]. The electron wave function at the exit of a QPC is written as

$$\Psi_0(0, y) = \left(\frac{2}{W}\right)^{1/2} \cos\left(\frac{\pi y}{W}\right) \quad \text{for } -W/2 \le y \le W/2, \quad (1)$$

and zero elsewhere, if the QPC carries only one conducting mode (cf. Fig. 1b). W denotes the QPC width at the exit. Using Green's theorem with Dirichlet's boundary

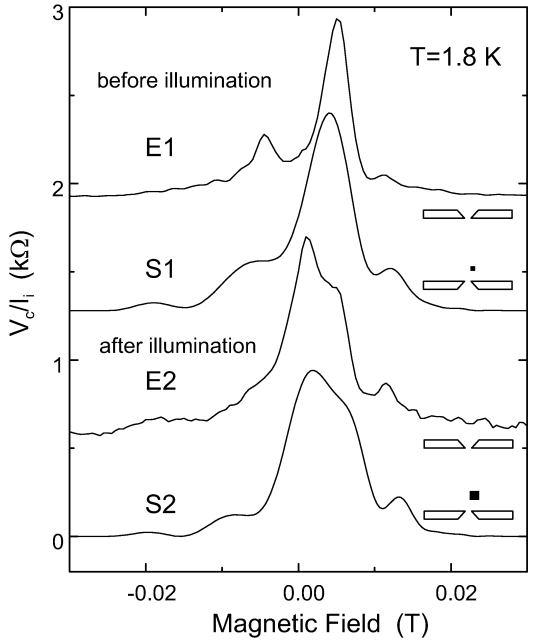

FIG. 3. Experiment (E) and simulation (S) of the collimation signal before (1) and after illumination (2). The fit parameters for traces $S1$ and $S2$ are $L_i = 0.65$ μm, $0.08 \leq y_i \leq 0.16$ μm and $L_i = 0.65$ μm, $0.08 \leq y_i \leq 0.22$ μm, respectively.

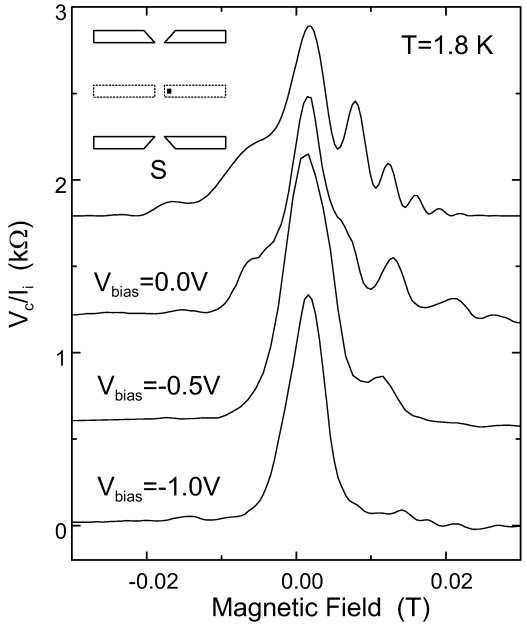

FIG. 4. Experiment and simulation (S) of the collimation signal for the bias-cooling experiment. The applied voltages are indicated in the figure. The fit parameter for trace S is $L_i = 2.00$ μm and $0.18 \leq y_i \leq 0.23$ μm.

conditions the wave function can be calculated for any point of the half plane ($x > 0$):

$$\Psi(\mathbf{r}') = \frac{i}{2m^*} \int_S dS\, \mathbf{n}(\mathbf{r}) [\Psi(\mathbf{r})\, (-i\hbar\nabla_{\mathbf{r}}) G^+(\mathbf{r}', \mathbf{r})]. \quad (2)$$

G^+, the Green's function in a weak magnetic field, which can be approximated by the Green's function at zero field, $G^0(\mathbf{r}', \mathbf{r})$, and a phase factor, $\theta(\mathbf{r}', \mathbf{r})$:

$$G^+(\mathbf{r}', \mathbf{r}) \simeq e^{i\theta(\mathbf{r}', \mathbf{r})}\, G^0(\mathbf{r}', \mathbf{r}), \quad (3)$$

$$\theta(\mathbf{r}', \mathbf{r}) = -\frac{e}{\hbar} \int \mathbf{A}(\mathbf{R}(t)) \frac{\nabla_{\mathbf{R}} G^0(\mathbf{R}(t), \mathbf{r})}{|\nabla_{\mathbf{R}} G^0(\mathbf{R}(t), \mathbf{r})|}\, dt, \quad (4)$$

a line integral along the gradient of $G^0(\mathbf{r}', \mathbf{r})$. For a detailed description of this method we refer to Ref. [15]. The wave function in the detector QPC, $\Psi_D(L, y)$, at a distance $x = L$ can be written analogous to Eq. (1). The transmission coefficient of the overall device can then be evaluated from

$$T = \left| \int_{-W/2}^{W/2} \Psi_D^*(L, y') \Psi(L, y')\, dy' \right|^2. \quad (5)$$

In order to simulate impurities, an intermediate line is introduced between injector and detector, ($0 < x = L_i < L$). The wave function Ψ_i is calculated at this line. The simplest model for the effect of a scattering object on the electronic wave function is just to set a part of the wave function Ψ_i to zero (cf. Fig. 1b). This modified wave function is then propagated further to calculate Ψ_D; Eq. (5) then gives the transmission probability. Of course, there are some limitations for the validity of the model: (i) Cutting off parts of a wave function is a very crude method to simulate scattering. Neither diffusive backscattering or forward scattering nor wave function matching at the boundaries is considered. However, this approximation is to a large extent justified by the finite dephasing length at our experimental conditions ($T \geq 1.8$ K); scattered electrons have lost their coherence when finally reaching the detector. (ii) The model neglects the strong collimation effect at $N = 1$. The Green's function expands in the full half-space behind the injector, leading to a broadening of interference features in the simulation. (iii) This type of modeling can never yield totally unambiguous solutions. The scatterer configurations given as the insets in Figs. 2, 3, and 4 are those with the smallest number of scatterers yielding simulations that satisfactorily reproduce the experiment. "Satisfactorily" here implies that the magnetic field values as well as the amplitudes of the fringes on the main collimation signal are recovered, and that adding an extra scatterer does not improve the agreement with experiment in any drastic manner. The simulated traces strongly depend on the actual impurity configuration, already a small variation of the size or location has a drastic effect on the observed interference patterns. From comparing the numerical results we estimate the uncertainty of the fitted values for L_i and W_i —within our model—as less than 5%.

What we cannot expect to recover from our modeling is the broadening of fringes [because of our neglect of the collimation effect, (ii)], as well as higher field structures as those of Fig. 2 at -25 mT, which occur only for one field direction. Such features can be modeled only by

incorporating multiple scattering, which is radically neglected here, (i). Within these limitations, we find that our model reproduces the experimental features remarkably well, cf. Figs. 2, 3, and 4. The main conclusion, however, that we draw from our modeling is that the observed fringes apparently result from only a few scattering centers, whose dimensions are in the 20 to 150 nm range.

Next, we discuss experiments that prove that the diffracting objects are due to the correlations in the distribution of donor states. Figure 3, trace $E1$, shows the observed interference pattern for a sample cooled down in the dark. At 1.8 K the QPCs were defined and the collimation signal was measured. The simulation yielded a width of $W_{i,S1} = 0.08$ μm in a distance $L_{i,S1} = 0.65$ μm. Subsequently, the device was illuminated using a 100 μs light pulse of a red light-emitting diode ($\lambda = 670$ nm) close to the sample. The resulting interference pattern differs significantly from the initial (Fig. 3, trace $E2$). Within the model for DX-center formation described above, this change can be attributed to a light-induced transformation of donors from the DX^- state into the d^+ state. At the same time the sample exhibits a slight increase in the carrier density, in good agreement with a $DX^- \rightarrow d^+$ conversion. From the simulation $S2$ an increase in the width of the scattering potential is found ($W_{i,S2} = 0.14$ μm). The observed change in the interference pattern of the electron beam is direct evidence for a reconfiguration of the scattering potential in the vicinity of the electron beam.

In Fig. 4 experimental curves are shown for a sample with an extra pair of gates between injector and detector. As indicated in Fig. 1a, these intermediate gates have a small gap of approximately 300 nm centered at the line connecting injector and detector. The collimation signal of this sample, cooled down without the intermediate gates defined, exhibits a distinct interference pattern. The simulation S reveals a scattering potential in the vicinity of the electron beam just underneath the intermediate gate ($L_i = 2.00$ μm and $0.18 \leq y_i \leq 0.23$ μm) for $V_{\text{bias}} = 0$ V. As demonstrated in Ref. [6] one may suppress the formation of DX centers by depleting the 2DEG through the application of a negative bias voltage at high temperatures. Below $T = 130$ K this (uncorrelated) donor configuration will be stable against thermal activation and the bias voltage can be released. The interference patterns resulting from applying exactly this procedure to intermediate gates are shown in Fig. 4 for $V_{\text{bias}} = -0.5$ and -1.0 V. The initial interferences are suppressed with increasing negative bias voltage. This can be understood by considering that the applied bias voltage suppresses the formation of DX^- centers underneath the gates, leading to a smoothening of the potential landscape in these regions. The experiments, Figs. 3 and 4, thus yield conclusive evidence that the observed interference patterns are indeed related to correlations in the donor state distribution.

In conclusion, electron-beam experiments probe directly the existence of long range correlations between donors in GaAs-(Al,Ga)As heterostructure on a microscopic level. Using a numerical method to simulate scattering potentials in the path of the electron beam in the 2DEG layer, it proves possible to deduce the position and size of scattering potentials by fitting an experimentally obtained interference pattern of an electron-beam signal. The typical size of the scatterers (20–150 nm) implies a collective effect of randomly distributed donors. This distribution can be changed by reducing the number of DX^- centers through illumination and bias-cooling techniques. The experiments show that a collimated electron beam is a sensitive tool in the investigation of local potential fluctuations in a 2DEG. For further study, it would be of interest to develop a more sophisticated theory of electron-beam scattering. Simulations using such a theory could in combination with, e.g., density-dependent experiments on the interference structures be used to yield a detailed picture of the shape and size of the density fluctuations in a 2DEG.

[1] T. Saku, Y. Horikoshi, and Y. Tokura, Jpn. J. Appl. Phys. **35**, 34 (1996).

[2] V. Umansky, R. de-Picciotto, and M. Heiblum, Appl. Phys. Lett. **71**, 683 (1997).

[3] J. A. Nixon and J. H. Davies, Phys. Rev. B **41**, 7929 (1990).

[4] A. L. Efros, F. G. Pikus, and G. G. Samsonidze, Phys. Rev. B **41**, 8295 (1990).

[5] P. T. Coleridge, Phys. Rev. B **44**, 3793 (1991).

[6] E. Buks, M. Heiblum, and H. Shtrikman, Phys. Rev. B **49**, 14 790 (1994).

[7] D. J. Chadi and K. J. Chang, Phys. Rev. Lett. **61**, 873 (1998); Phys. Rev. B **39**, 10 063 (1989).

[8] H. J. Queisser and E. E. Haller, Science **281**, 945 (1998).

[9] S. Bednarek and J. Adamowski, Phys. Rev. B **55**, 2195 (1997).

[10] R. Fletcher *et al.*, Phys. Rev. B **41**, 10 649 (1990).

[11] M. Hayne *et al.*, Phys. Rev. B **57**, 14 813 (1998).

[12] A. R. Long *et al.*, Semicond. Sci. Technol. **8**, 1581 (1993).

[13] E. Skuras *et al.*, Semicond. Sci. Technol. **10**, 922 (1995).

[14] P. T. Coleridge, Semicond. Sci. Technol. **12**, 22 (1997).

[15] M. Saito, M. Takatsu, M. Okada, and N. Yokoyama, Phys. Rev. B **46**, 13 220 (1992).

[16] L. W. Molenkamp *et al.*, Phys. Rev. B **41**, 1274 (1990).

[17] M. Okada *et al.*, Superlattices Microstruct. **10**, 493 (1991). These authors report on a splitting in the electron beam signal which is attributed to diffraction of the beam at the QPC exit. However, as shown in [16], the QPC potential is smooth. Based on the results reported here, we suggest that these observations have a similar origin as discussed in the present paper.

[18] K. L. Shepard, M. L. Roukes, and B. P. van der Gaag, Phys. Rev. B **46**, 9648 (1992); J. Appenzeller, Ph.D. thesis, Berichte des Forschungszentrums Jülich, Jül-3080, 1995; G. Timp, in *Semiconductors and Semimetals*, edited by M. Reed (Academic Press, New York, 1992), Vol. 35, p. 113.